

LOW-MASS SUBSTELLAR CANDIDATES IN NGC 2264

TIM KENDALL¹, JEROME BOUVIER¹, ESTELLE MORAUX² and DAVID JAMES³



1. *Laboratoire d'Astrophysique de Grenoble, BP 53X, 38041 Grenoble Cedex, France*

2. *Institute of Astronomy, University of Cambridge, Madingley Road, Cambridge, CB3 0HA, UK*

3. *Physics & Astronomy Dept., Vanderbilt University, 1807 Station B, Nashville, TN 37235 USA*

NGC 2264 is a young (3 Myr), populous star forming region for which our optical studies have revealed a very high density of potential brown dwarf (BD) candidates - 236 in $< 1 \text{ deg}^2$ - from the substellar limit down to $\sim 20 M_{\text{Jup}}$. Candidate BD were first selected using wide field (I;z) band imaging with CFHT/12K, by reference to current theoretical isochrones. Subsequently, around 50% of the I;z sample were found to have near-infrared (2MASS) photometry, allowing further selection by comparison with the location of DUSTY isochrones in colour-colour diagrams involving combinations of I,J,H and K colours. After rejection of objects with only upper limits to J, six candidates were selected from the I K ;J H diagram which afforded the best separation of candidate and field objects; of these, 2 also lie close to the model predictions in the I J;I K and I J;H K plots. After dereddening, all six remain probable very low-mass NGC 2264 members, in spite of their low A_v , while a different group of objects are shown to be highly reddened background giants. A further three brighter (at I) objects selected by their I J;I K colours, lie at the substellar limit and are likely cluster objects, as are 2 intermediate mass objects selected by their I K and H K colours. These objects potentially constitute a hitherto unknown population of young, low-mass BD in this region; only slightly deeper observations could reveal a new laboratory for the study of near-planetary-mass objects.

Keywords: stars: low mass, brown dwarfs – infrared: stars – surveys – Galaxy: open clusters and associations

1 Introduction

Within the last few years the observational study of substellar objects ($M < 0.072 M_{\odot}$) has undergone spectacular and rapid development, opening up new perspectives on the formation of such objects within molecular clouds. Large numbers of BD have now been found in star-forming regions, young clusters and the field^{1;2;3;4} and physical models of the atmospheres of BD constructed^{5;6}, opening up the possibility of confrontation between observations and theoretical predictions of the physical properties of BD. However, the core issues of the form of the substellar initial mass function (IMF) and its dependence on environment remain to be addressed. The discovery of BD in widely differing environments does suggest their formation is directly linked to the star formation process, and early estimates of the substellar IMF in the solar neighbourhood have indicated that BD are nearly as numerous as stars. Within this broad framework, two competing scenarios have been put forward for BD formation; the first simply that they form as stars do, i.e. by the gravitational collapse of low mass molecular cloud cores⁷; the second postulates the dynamical ejection of the lowest mass protostars, leading to BD formation since the ejected fragments are unable to further accrete⁸. To distinguish between these possibilities and to obtain unbiased

estimates of the substellar IMF, observations of statistically complete, homogeneous populations of BD are needed in a wide variety of environments with different ages. Such a deep, wide-field imaging survey has been performed in the $I; z$ bands with CFHT/12K/MegaCam: “Brown dwarfs and the substellar mass function: Clues to the star formation process”, initiated by J. Bouvier and collaborators.

The study of NGC 2264 introduced here is only a small part (0.6 deg^2) of the whole survey, which, for the first time, has covered significant areas (70 deg^2) of star-forming environments, pre-main sequence clusters and older open clusters (ages 1–600 Myr) with the aim of reaching $I = 24$ which corresponds to $25 M_{\text{Jup}}$ at the distance of Taurus (140 pc) for age 10 Myr and extinction $A_v = 10 \text{ mag}$; in all of the targeted regions, the limiting mass is in the range $10\text{--}40 M_{\text{Jup}}$ and NGC 2264, because of its youth and relative proximity (3 Myr, 770 pc^{9;10}), is probed to the lower end of this mass range with the current observations.

2 Young brown dwarfs in star-forming regions (SFRs)

Young BD (with ages 1–3 Myr) are now being uncovered (for a recent compilation see¹¹) but the census remains very incomplete to date. The CFHT project as a whole has now discovered a substantial sample of candidate young substellar objects - several hundred to date - which can be studied statistically with confidence and which can provide targets for observations in other wavelength regimes (eg. with the Spitzer Telescope). The youth of such objects ensures that their population has not yet suffered from important dynamical (and stellar) evolution, other than dynamical effects potentially associated with their formation. This is a point worth underlining, since observations of young SFRs have the potential to distinguish the two BD formation mechanisms outlined in Sect. 1 by their resultant spatial distributions. If BD always form exactly as stars do, one would expect them to trace the regions of the highest density of low-mass stars. However, in any dynamical ejection scenario, a deficit of BD may be expected in the central regions of young star-forming clusters; their initial velocities ($\sim 1 \text{ km s}^{-1}$)¹² moving them away from their birth sites at $\sim 0.3 \text{ /Myr}$ (at 140 pc). Such a deficit would therefore be observable in all nearby young SFRs.

Comparison with young SFRs with a range of environmental conditions (from the low density regions such as Taurus to regions where stars are forming in very massive clusters, such as Upper Scorpius) also permits investigation of the sensitivity of the low-mass end of the IMF to local conditions. Sufficiently large coeval populations are not yet available to perform such studies with confidence, but recent studies are beginning to address such questions. As an example, 30 substellar candidates have been identified in Taurus in a 3.6 deg^2 region using CFHT/12K data which reached to $I = 23.5$. Spectroscopic follow-up led to the identification of four BD in Taurus¹³ with spectral types later than M7. In Taurus, ~ 10 BD are now known¹⁴, and appear to be spatially correlated with regions of highest stellar density. In Upper Scorpius, initial studies¹⁵ have found 18 candidate BD of which 5 show signs of ongoing accretion. We will compare our initial findings on NGC 2264 in Sect. 4; here we will note that the much larger BD populations being uncovered by CFHT/12K, when fully analysed, promise a more robust statistical treatment of these issues.

3 Candidate NGC 2264 brown dwarfs: Optical and near-infrared colour selection

The pre-reduction and analysis of these data have been performed using CFHT Elixir pipelines^a and innovative point-spread function fitting techniques developed by E. Bertin at the Institut d’Astrophysique de Paris^b. Full details of these methods will be published in a later paper. A first selection of candidates was made by choosing those redder than the long dashed line in Fig. 1., which shows optically selected candidates in NGC 2264 between the substellar limit and $\sim 10 M_{\text{Jup}}$, by comparison with the state-of-the-art DUSTY models, specially created by Baraffe et al. to take account of the CFHT $I; z$ filter responses (see⁵ and references therein for full details of these models). All 236 such $I; z$ candidates (squares in Fig. 1) have been visually inspected on both I and z frames and all found to be stellar in nature, i.e. there are no artifacts due to nebulosity, field edges, bad columns, bright stars etc. As can be seen in Fig. 1, we estimate our data are complete to $I = 22$, or $12 M_{\text{Jup}}$ for age 2 Myr. Cross-correlation with the 2MASS all sky release data has yielded 101 counterparts to the $I; z$ candidates with $J; H; K$ magnitudes accurate to ~ 0.3 magnitudes or better (a further 29 have only upper limits to J (and for 5, K)). These counterparts are plotted in Fig. 2(a) as large squares, together with the complete set of 2MASS data within the optically surveyed area (crosses), in the $I - K; J - H$ colour-colour diagram. It is clear that this diagram provides

^awww.cfht.hawaii.edu

^bwww.terapix.iap.fr

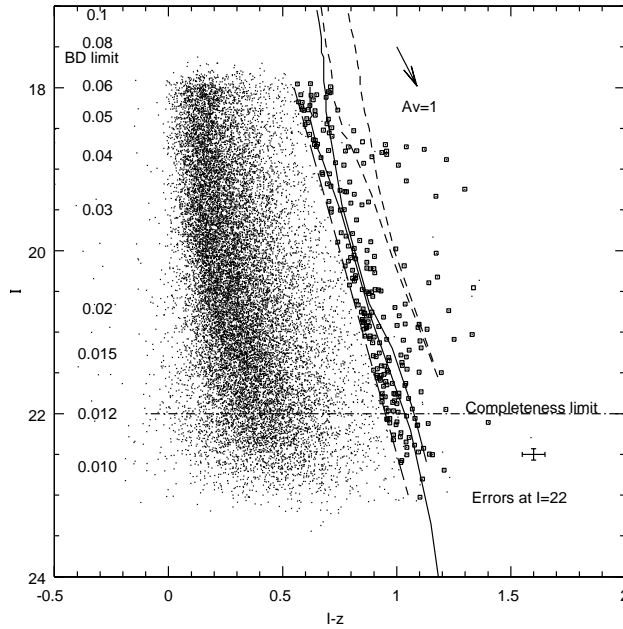


Figure 1: $(I, I - z)$ colour-magnitude diagram built using long (360 sec) exposures of NGC 2264. The solid isochrones are DUSTY models for an ages 2 and 5 Myr; the dashed isochrones are the NextGen models at the same ages. All isochrones are for a distance of 770 pc. 236 BD candidates (squares) were selected to be redward of the sloping straight line (long dash). Small dots redward of this line were rejected from the candidacy on visual inspection. The mass scale (in M_{\odot}) is for the 2 Myr models; it and the estimated completeness limit are indicated.

an excellent separation between candidates and field objects. A number of candidates are extremely red, with $I - K \approx 6$ and $I - J \approx 3-4$; the latter colour being typical of field objects with late M or L spectral types, e.g. ¹⁶.

To further refine our sample, we have followed similar methods to those of ^{14, 17} in Taurus, using combinations of $I; J; H; K$ colour-colour diagrams to select those optical candidates which lie on or close to the model isochrones in these diagrams. For the similarly young and extinction affected NGC 2264 region, our finding that the $I - K; J - H$ diagram yields the best separation between field 2MASS objects and candidate BD is in agreement with these authors. In practice, we have chosen candidates lying close to the isochrone in Fig. 2(a), after discarding $I; z$ candidates with only upper limits to J or K . Fig. 2(b) shows objects selected in various colour combinations (see key) re-plotted in the $I; I - z$ diagram, and, in Fig. 3(a), the $I - K; J - H$ diagram. It can be clearly seen that objects selected by $I - J; H - K$ colours *only* (open squares in Figs. 2(b) and 3(a)) do not as a group fall close to the cluster isochrones in $I; I - z$ and these objects are almost certainly reddened background giants. Indeed, in a conventional $JH - K$ colour-colour diagram (Fig. 3(b)) many objects *only* selected by their $I - J; H - K$ colours lie within the reddening band. However, candidates selected in the $I - J; I - K$ and, especially, $I - K; J - H$ diagrams, tend to lie away from the reddening band, and closer to the cluster isochrone. They can therefore be considered much more likely to be substellar NGC 2264 members. Such candidates are plotted by small open squares and open hexagons in Figs. 2(b) and 3.

These arguments are backed up by simple dereddening in $J - H$ where all objects have been taken to the low-mass tip of the dwarf sequence in Fig. 3(b), and subsequently replotted in the $I; I - z$ diagram (Fig. 4(a)). To deredden z , we interpolate the interstellar reddening laws of ¹⁸ to find $A_z/A_v = 0.406$, taking the optimum sensitivity of the z filter at 9800\AA , as given by the CFHT website. As a group, the $I - J; H - K$ selected objects are proven to be highly reddened with A_v ranging up to ≈ 1.7 . Only one such object might be considered a member by reference to its position near the tip of the 2 Myr isochrone in $I; I - z$; one further candidate is simultaneously selected in $I - J; I - K$ and has a predicted mass near $40 M_{Jup}$. Six objects, all part of the $I - K; J - H$ selection, lie close to the isochrones with masses ranging down to $20 M_{Jup}$, and three more chosen by their $I - J; I - K$ colours only are clustered near the model predictions very close to the BD limit. Therefore, the total number of probable substellar members found in NGC 2264 and reported here is eleven.

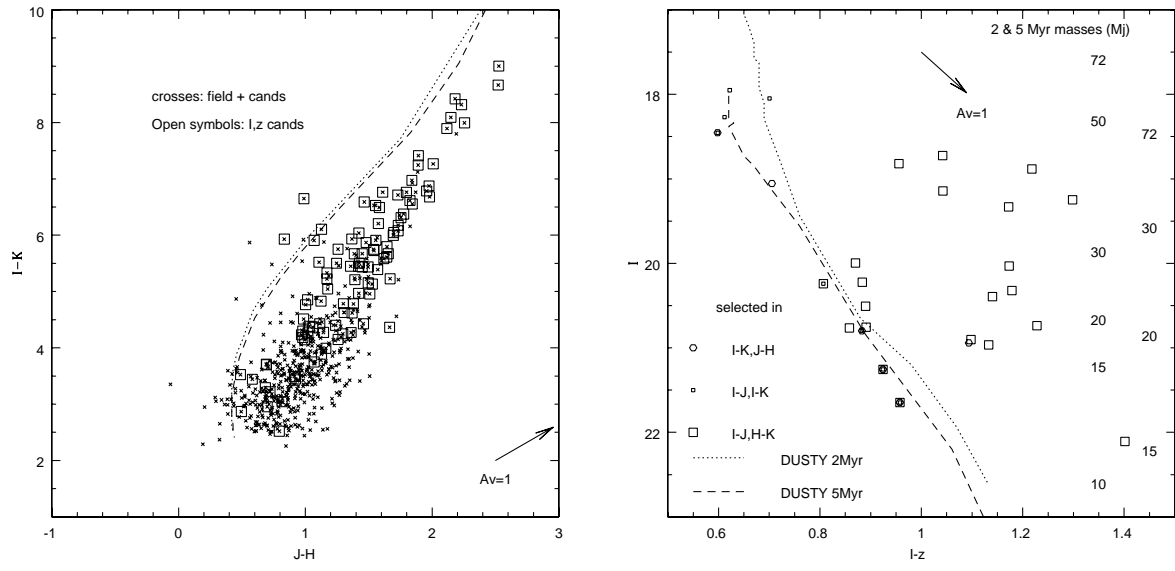


Figure 2: (a, Left): All $I-z$ candidates with 2MASS (squares) and all 2MASS points (field and candidates, crosses) in the $I-K; J-H$ colour-colour diagram. Note the separation of the two populations and the reddening vector. The dashed curve is the 5 Myr DUSTY isochrone; the dotted, 1 Myr. Figure 2: (b, Right): Final selection of candidates from colour indices in $I; J; H; K$, plotted in the $(I; I-z)$ diagram, and excluding objects with only $J; K$ upper limits. It is clear that the the $H-K$ colour is least efficient at selecting objects near the model loci. DUSTY isochrones only are plotted as in Fig. 1. Candidates were selected from their locations in the $I-K; J-H$ diagram *and* two other colour combinations (see key). Typical errors in I and $I-z$ are small, ~ 0.1 mag. (see Fig. 1).

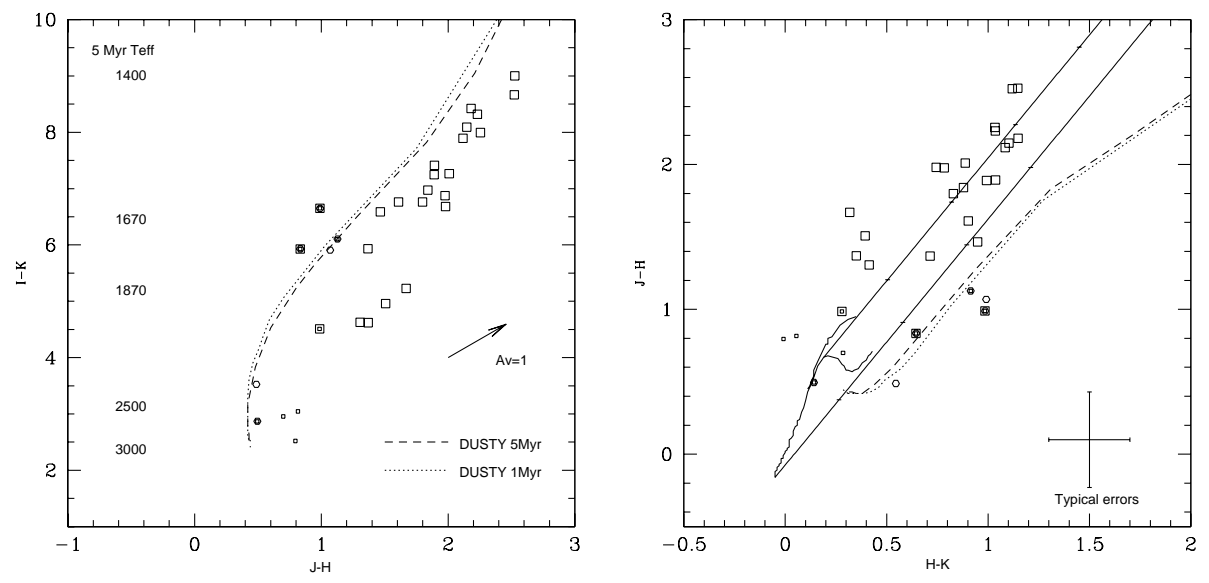


Figure 3: (a, Left): Final census of near-infrared selected objects plotted in the $I-K; J-H$ diagram, as an aid to visualizing the selection space. Note the T_e scale based on $I-K$ colour. Figure 3: (b, Right): Location in the $J; H; K$ diagram. The reddening band (RB) is shown (each horizontal tickmark represents $A_v = 5$), together with loci for dwarfs and giants. Objects selected only in $I; J; H; K$ are clearly more likely to be reddened contaminants; the most promising candidates lie away from the RB and close to the DUSTY isochrones in this plot. Some may have small K -band excesses. 1 and 5 Myr DUSTY isochrones are plotted as for Fig. 3(a). Typical 2MASS errors are given; the error in $I-K$ is somewhat smaller than in $J-H$ or $H-K$, as it is dominated by that in K and the error in I from our 12K data is comparatively small.

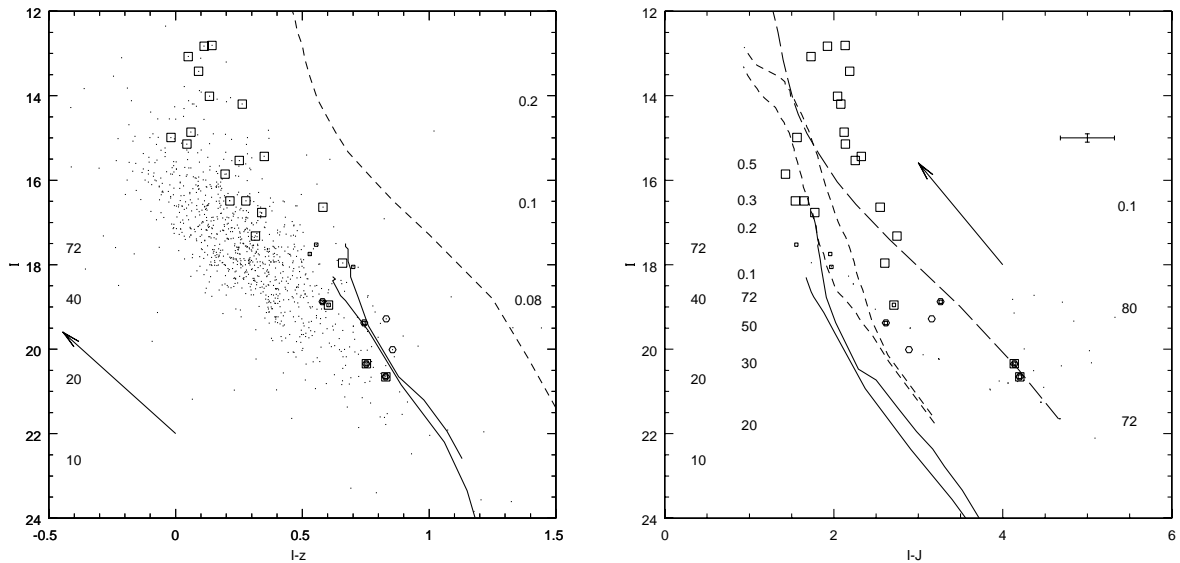


Figure 4: (a, Left): Locations of objects in $I; I - z$ after simple dereddening described in the text. Most $H - K$ selected objects (open squares) are clearly in the background. The dots are a locus of *all* 2MASS points in the region, similarly dereddened; the locus of all field points. The best cluster candidates selected by the methods described here lie noticeably away from this locus. The arrow represents the dereddening vector for $A_v = 5$. 2 and 5 Myr DUSTY isochrones are plotted as solid curves for which the mass scale at left is for 2 Myr; the dash is the location of a 5 Gyr isochrone, representing the field, at 60 pc. (b, Right): As Fig. 4(a) but for $I; I - J$. DUSTY isochrones are solid curves, short dashes NextGen, for 1 and 5 Myr ages. The long dash is the field isochrone for 60 pc. Dots are locations before dereddening. Mass scales are for the 5 Myr DUSTY (extreme left), 2 Myr NextGen (left) and the field model (right). The possibility that the two points lying on it at $\sim 75 M_{\text{Jup}}$ are *foreground field objects* is discussed in the text. A typical errorbar is shown.

4 Discussion and concluding remarks

The first and most important point concerns the masses of our candidates, derived from their I magnitudes after dereddening, by comparison with theoretical models for 2 and 5 Myr plotted for a distance modulus 9.4. For the 11 most probable cluster members shown in Fig. 4(a) and discussed above, predicted masses range between the substellar limit and close to $20 M_{\text{Jup}}$.

However we caution that the photometric methods used in this work do not rule out that some of the candidate BD may be background giant or faint foreground contaminants. This is an important point, in the light of the obvious existence of strong and variable extinction intrinsic to the NGC 2264 region itself as discussed at length by ¹⁰ (and references therein), and in the foreground, since the region lies close to the galactic plane. Clearly, our methods can distinguish background giants. However, ¹⁰ draw attention to the surprising fact that a number of *known* NGC 2264 members exhibit only the reddening expected in this line of sight at $b=2$, $E_{B-V} = 0.5$. Presumably, these members must lie on the near edge of the cloud and be unaffected by reddening intrinsic to the cluster nebulosity itself. The eleven objects suggested here as substellar members have A_v typically in the range 0–3 and *not more than 4*, as apart from the objects we have clearly identified as background giants suffering 15 magnitudes of extinction. Their A_v are therefore perfectly consistent with cluster membership, although they may be preferentially located on the near edge of the cloud.

This discussion brings to the point the question of contamination by *foreground* objects. It is seen from inspection of the $I; I - J$ diagram in Fig. 4(b) that the candidates are spread in colour between the cluster models and an isochrone plotted for age 5 Gyr (i.e. representing the *field* population) at a distance chosen to be 60 pc to bisect the two candidates selected in all colours and shown as triply overplotted points. For reasons which we defer to a future paper, the question of foreground contamination is not raised by the location of the same isochrone in $I; I - z$ (Fig. 4(a)). However, the status of these 2 objects in particular, as questioned by their dereddened $I - J$ colour, can be further investigated. These objects have A_v of 1.25 and 2.7, as determined by our method. At first sight, it would appear that it is very unlikely that a foreground object at 60 pc would suffer such extinction, supporting the claim that they are true NGC 2264 members with masses not near the BD limit but instead much lower. Indeed, for one of these objects the 2MASS J -magnitude is flagged “D” and its $I - J$ colour might be bluer

(nearer the cluster isochrone) than plotted; the other is flagged “C” and may also be bluer by at least the typical error shown in Fig. 4(b).

Further general arguments favourable to the identification of these eleven candidates as NGC 2264 members are provided by the observation of clear separation of $I; z$ selected objects from the field in the $I_K; J_H$ diagram and by the classical $J_H; H_K$ diagram (Fig. 3(b)), in which the location of DUSTY isochrones has *not* been employed for candidate selection. It can be readily seen that, even before any dereddening, the best candidates as a group here lie away from the reddening band, while other initially plausible candidates, selected using their I_J and H_K colours only, are more scattered over the diagram, often lying within the reddening band. A similar separation identifies background giants in the dereddened $I; I_z$ plot. Such observations further strengthen the effectiveness of our photometric selection methods, with $I_K; J_H$ selected candidates preferentially located closest to the DUSTY isochrones in all colour-colour and colour-magnitude diagrams. The location of a few candidates in $J_H K$ also raises the possibility that they have K -band excesses, which might indicate ongoing accretion, and can be tested first by photometric observations in the thermal infrared with Spitzer. Current studies do not easily show whether the presence of disks might be still expected around young BD at the age of NGC 2264, and our candidates provide a good opportunity to constrain disk ages in this way.

It is clear however that near-infrared spectroscopy is also required to confirm candidates on the basis of their T_e and surface gravities, which will be significantly less than foreground, evolved field objects owing to the young age of the region.

In conclusion, there is a strong likelihood that our preliminary work has indeed uncovered a small initial sample of low mass brown dwarfs, some of which may have masses only twice the deuterium burning limit. Deeper near-infrared photometry than given by 2MASS is likely to identify more of our $I; z$ candidates as near-planetary mass BD. If so, then NGC 2264 will prove to be a new astrophysical laboratory, intermediate in stellar density between Orion and Taurus, where the formation mechanisms of such objects in star-forming environments can be investigated.

Acknowledgments

TRK and DJJ acknowledge support from the 5th Framework European Union Research Training Network “The Formation and Evolution of Young Stellar Clusters” (RTN1-1999-00436) and TRK from the French *Ministère de Recherche*. EM acknowledges support from PPARC.

References

1. Bejar, V.J.S., Martín, E.L., Zapatero-Osorio, M.R., et al. 2001, *ApJ*, 556, 830
2. Moraux, E., Bouvier, J., Stauffer, J.R., & Cuillandre, J.-C. 2003, *A&A*, 400, 891
3. Chabrier, G. 2002, *ApJ*, 567, 404
4. Chabrier, G. 2003, *PASP*, 115, 763
5. Baraffe, I., Chabrier, G., Barman, T.S., et al. 2003, *A&A*, 402, 701
6. Chabrier, G., et al., 2000, *ApJ*, 542, 464
7. Padoan, P., & Nordlund, A. 2002, *ApJ*, 576, 870
8. Reipurth, B., & Clarke, C. 2001, *AJ*, 122, 432
9. Lamm, M.H., Bailer-Jones, C.A.L., Mundt, R., et al. 2004, *A&A*, 417, 557
10. Rebull, L.M., Makidon, R.B., Strom, S.E., et al. 2002, *AJ*, 123, 1528
11. Basri, G. 2000, *ARA&A*, 38, 485
12. Sterzik, M.F., & Durisen, R.H. 2003, *A&A*, 400, 1031
13. Martín, E.L., Dougados, C., Magnier, E., et al. 2001, *ApJ*, 561, L195
14. Briceno, C., Luhman, K.L., Hartmann, L., et al. 2002, *ApJ*, 580, 317
15. Martín, E.L., Delfosse, X., & Guieu, S. 2004, *AJ*, 127, 449
16. Kendall, T.R., Delfosse, X., Martín, E.L., & Forveille, T. 2004, *A&A*, 416, L17
17. Luhman, K.L., Briceno, C., Stauffer, J.R., et al. 2003, *ApJ*, 590, 348
18. Rieke, G.H., & Lebovsky, M.J., 1985, *ApJ*, 288, 618